JOURNAL OF GEOPHYSICAL RESEARCH, VOL. 105, NO. D2, PAGES 2281–2290, JANUARY 27, 2000

Mountain reference technique: Use of mountain returns to calibrate weather radars operating at attenuating wavelengths

Soumia Serrar, Guy Delrieu, Jean-Dominique Creutin, and Remko Uijlenhoet
Laboratoire d'Étude des Transferts en Hydrologie et Environnement, Grenoble, France

Abstract. The Mountain Reference Technique (MRT) was proposed as a means to perform a self-calibration of a weather radar system operating at an attenuating wavelength in a mountainous environment. Two convective rain events observed during the Grenoble 97–98 Experiment are selected here for an illustration and a further verification of the method at X band: the June 16, 1997, event is a medium event with maximum path-integrated attenuations (PIAs) of about 15 dB over a 9-km path, while the July 3, 1998, event is quite extraordinary with (1) a maximum PIA of 50 dB over the same distance and (2) the temporary presence of hail. An improved scheme is proposed for the MRT parameter estimation procedure with a more satisfactory treatment of such high-attenuation effects. It is shown that the optimal calibration factors obtained for the two rain events are almost equal to each other, a comforting result with respect to the radar equipment stability during the corresponding 1-year period. Although the MRT is based on reflectivity and attenuation measurements only, validation of the rain rate retrieval algorithms with respect to rain gage data for the June 16, 1997, rain event showed that this technique is relevant in terms of rain rate estimation. In particular, the MRT-calibrated Hitschfeld-Bordan algorithm provides satisfactory results for this medium-attenuation event. However, the July 3 case clearly demonstrates that this algorithm cannot correct for such high-attenuation effects because of its inherent instability. For both rain events the Marzoug-Amayenc algorithm, originally proposed for spaceborne configurations, is found to be stable and efficient in terms of rain rate estimation. These interesting features are counterbalanced by the fact that the algorithm implementation is limited to directions for which PIA measurements are actually available.

1. Introduction

The term "Mountain Reference Technique" (MRT) clearly refers to the surface reference technique proposed by *Meneghini et al.* [1983] for rainfall measurement at attenuating wavelengths in spaceborne radar configurations. The latter concept is based on the estimation of path-integrated attenuations (PIAs) from the difference between Earth surface returns in the presence and in the absence of rain. These measurements can be used in various ways to estimate the average rain rate over the propagation path or to constrain rain rate profiling algorithms [*Marzoug and Amayenc*, 1994]. Feasibility of applying this technique to ground-based attenuated weather radar systems operating in mountainous regions was already demonstrated within the Marseille 92–93 Hydrometeorological Experiment devoted to the improvement of rain measurement and prediction techniques for urban hydrology applications [*Delrieu et al.*, 1997 (hereinafter referred to as DCC97)]. In this context the radar siting and the scan strategy of the LTHE X-band light configuration radar were defined to obtain both (1) short-range rain reflectivity measurements free of ground detection over a large domain at a medium-elevation angle and (2) strong mountain returns at a low-elevation angle over an azimuthal sector of ~60°. From these returns, PIA estimates were derived and used to successfully process the upper elevation rain reflectivity data in terms of rain rate.

Paper number 1999JD901025.
0148-0227/00/1999JD901025$09.00

A specific experiment was conducted in 1997 and 1998 in Grenoble, France, to extend the preliminary results of the Marseille case study. The first aim of the Grenoble 97–98 Experiment was to assess the accuracy of the mountain-derived PIAs, a critical point for the considered method. This was done by operating an X-band receiving antenna in the Belledonne mountain ridge in relation with the LTHE X-band radar operating down in the Grésivaudan valley in range-height indicator (RHI) mode. The direct PIA measurements were compared to the PIA estimates given by the corresponding mountain returns. The interested readers are referred to *Delrieu et al.* [1999b] (hereinafter referred to as DSGC99) for a comprehensive presentation and discussion of the results obtained. As a brief summary, we may say that (1) the overall quality of the mountain PIA estimates is good with a standard error of ±2.5 dB in the considered configuration, (2) a minimum detectable PIA of about 2.2 dB results from the natural time variability of the dry-weather mountain returns, and (3) the negative bias in the PIA estimation due to the effects of rain falling over the reference target can be reduced by considering mountain targets with dry-weather apparent reflectivity as high as possible ("strong mountain returns" herein).

In the present paper, focus will be given to the second aim of the Grenoble 97–98 Experiment, i.e., a further verification of the MRT after DCC97. The data collected during two rain events of special interest, namely the June 16, 1997 and the July 3, 1998, rain events are presented in section 2. A brief review of the rain rate retrieval algorithms that can possibly be applied in the considered context is given in section 3. The

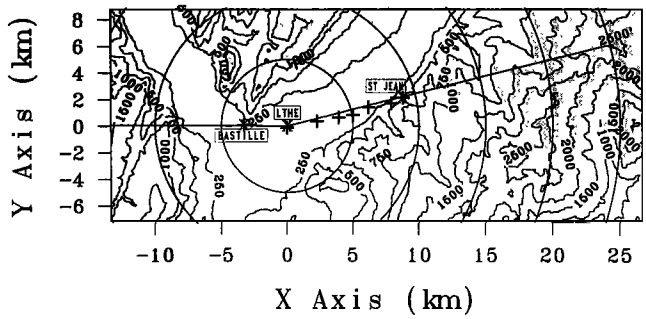

Figure 1. Presentation of the study area. A digitized terrain model (with 250-m isolines) of the Grenoble region is presented together with the locations of the measurement devices. The position of the X-band radar is indicated by a cross and 5-km range markers. In 1997 the radar was operated in range-height indicator (RHI) mode in the direction of Saint Jean where the receiving antenna (cross) was installed; the plus signs refer to the locations of the rain gages that were deployed along the 9-km propagation path for validation purposes. In 1998 the receiving antenna was set up at a closer range (Bastille site) with a rain gage network (plus) reduced to two devices, one at the radar site and the other at the receiving antenna site. During this second experiment, the radar was still operated in RHI mode.

MRT is presented in section 4 as a means to solve the radar calibration problem using radar data alone. Finally (section 5), a validation of the rain rate retrieval algorithms with respect to rain gage data is given for the two rain events together with the sensitivity of the results regarding the drop size distribution parameterization.

2. Data Set

Figure 1 presents the study area of the Grenoble 97–98 Experiment. The X-band radar (see DSGC99 for the main parameters of this radar system) was installed on the roof of the laboratory (Grenoble campus) at an altitude of 217 m above sea level (asl). In 1997 the radar was operated in RHI mode in the direction of Saint Jean le Vieux (hereinafter Saint Jean), a small village in the Balcons de Belledonne area, located at an altitude of 750 m asl and at a range of 9 km of the radar site. Direct PIA measurements were obtained in Saint Jean by means of an X-band receiving antenna. A network of seven tipping-bucket rain gages was installed along the propagation path for validation purposes. In 1998 a lighter measurement configuration was implemented with the receiving antenna installed at the "Institut de Géographie Alpine" (range 3 km, altitude 300 m asl) in the Bastille mountain that dominates the Grenoble city center. Two rain gages were also operated at the radar and the receiving antenna sites. Owing to the immediate environment of the radar site (forested area), the range r_0 for which reflectivities are contaminated by sidelobe effects is actually very small in the present situation. Range r_0 was taken equal to 625 and 375 m for the 1997 and 1998 configurations, respectively. Furthermore, in both configurations, two strong mountain clutters are available at average ranges denoted r_1 and r_2. These reference targets correspond to the Balcons de Belledonne area (r_1 = 8.5 km) and to the high tops of the Belledonne mountain (r_2 = 20 km) for the 1997 measurement configuration. For the 1998 configuration the first reference target is the Bastille mountain (r_1 = 3 km), and the second one corresponds to the Vercors mountain at a range r_2 = 9 km.

Figures 2 and 3 present the main characteristics of the data collected during the June 16, 1997 and the July 3, 1998 rain events. In these two figures the first two graphs display the radar measurables: the top graph is a range-time indicator (RTI) of the measured reflectivity profile $Z_m(r)$ (with standard units of mm^6/m^3) derived from the average backscattered

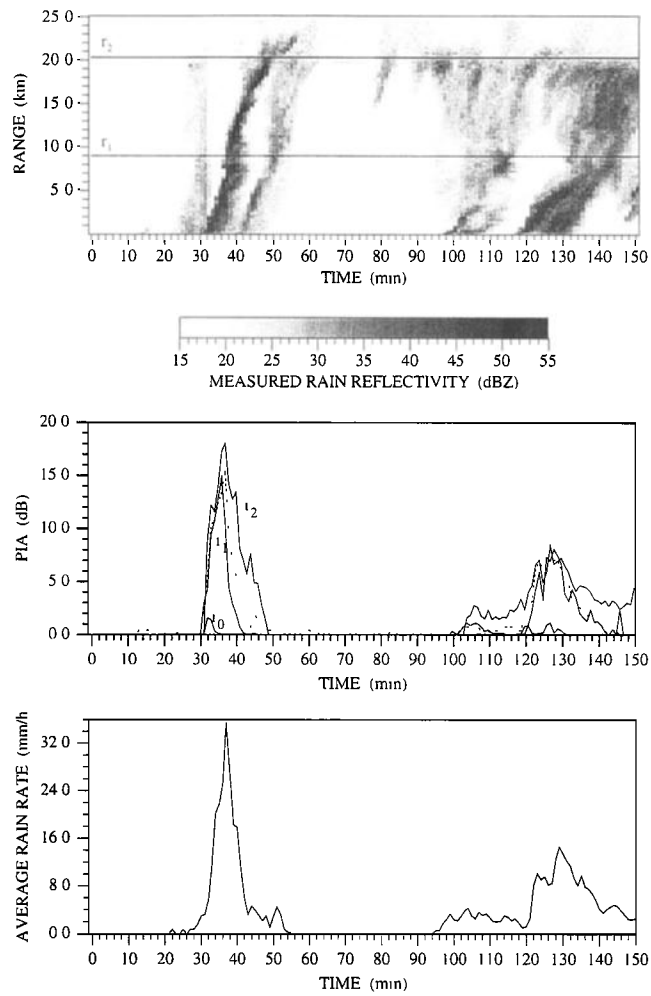

Figure 2. June 16, 1997, rain event displayed as a function of time. The top panel corresponds to the range-time indicator (RTI) of the measured rain reflectivity profile between the radar and the range 25 km in the direction of Saint Jean. At a given range the reflectivity measurements performed at the lowest elevation free of ground detection are extracted from the RHI to obtain the displayed RTI. The middle panel corresponds to the path-integrated attenuation (PIA) measurements at ranges r_0, r_1, and r_2. The close-range PIA (r_0 = 625 m), derived from (2) using a thunderstorm Z-k relation $Z = 163300k^{1.24}$, remains less than 1.5 dB. Mountain-derived PIAs at ranges r_1 and r_2 are calculated from the corresponding mountain returns using (3). For comparison the dashed line represents the PIA measured with the receiving antenna at range r_1. The main discrepancies between the two signals occur between time steps 39 and 41 corresponding to high rain rates over the receiving antenna site. The bottom graph presents the time evolution of the average rain rate between the radar and the range r_1 as derived from the rain gage network.

power profile $P(r)$ (mW) by means of the weather radar equation

$$Z_m(r) = P(r)r^2/C|K|^2, \quad (1)$$

where r (km) is the range of observation, and C is the radar constant for a weather target [*Doviak and Zrnic*, 1993]. This constant, subject to "electronic" calibration, depends on the radar parameters such as the peak power, wavelength, antenna beam and gain, pulse duration, etc. $|K|^2$ is another constant, equal to ~0.93 for water (the assumed value in (1)) and 0.18 for ice, which depends on the complex refractive index of the hydrometeors. The displayed $Z_m(r)$ values correspond to rain reflectivities since, at any range r, they are derived from the measurements performed at the lowest elevation angle free of ground detection. The middle graphs in Figures 2 and 3 give the time evolution of the PIAs estimated between the radar and the ranges r_0, r_1, and r_2, respectively. The close-range PIA (dB) at range r_0 was calculated using the following expression:

$$\mathrm{PIA}_m(r_0) = 2r_0\left(\frac{Z_0}{\alpha}\right)^{1/\beta}, \quad (2)$$

where Z_0 (mm^6 m^{-3}) is a measured reflectivity in the vicinity of the radar (which is between ranges r_0 and $r_0 + \Delta r$, with $\Delta r = 500$ m here), and α and β are the coefficients of a power-law relation between the reflectivity and the attenuation coefficient (see section 3). The mountain PIAs at ranges $r_M = r_1$ or r_2 were derived from the simple ratio of the average values of the apparent reflectivities of the mountain returns during rainy ($Z_R^M(r_M)$) and nonrainy ($Z_{nR}^M(r_M)$) conditions (DSGC99):

$$\mathrm{PIA}_m(r_M) = -10 \log (Z_R^M(r_M)/Z_{nR}^M(r_M)). \quad (3)$$

For range r_1 the PIA measured with the receiving antenna is displayed to allow a semiquantitative assessment of the mountain-PIA accuracy (note that the receiving antenna measurements are not used herein in the MRT implementation).

Finally, the bottom graphs in Figures 2 and 3 present the time evolution of the average rain rate value derived from the rain gage network (June 16, 1997, case) or the individual hyetographs (July 3, 1997 case) in order to show the magnitude of the rain events.

The June 16, 1997, rain event consisted of two rainy periods lasting 20 and 60 min, respectively. To the maximum average rain rate of about 35 mm h^{-1} over the 9-km propagation path corresponds a PIA of 15 dB at range r_1 during the first period. A maximum average rain rate of 15 mm h^{-1} corresponds to a PIA of 8 dB during the second one. This event, the most important of the 1997 measurement campaign in terms of PIA, was surpassed on July 3, 1998, since a PIA of 50 dB (!) has been measured at range $r_2 = 9.5$ km within a rainy period that lasted about 20 min. The Bastille hyetograph confirms, with rain rates >100 mm h^{-1} during 5 min, the importance of this event. Note also that the presence of hail was reported at ground level at the Bastille site at the beginning of the event. It should be recalled that 10–15 dB are probably the maximum PIA values [*Delrieu et al.*, 1999b] which can be corrected using standard algorithms [e.g., *Hitschfeld and Bordan*, 1954] owing to the instability of the equation describing attenuation effects. In this respect, the June 16, 1997, rain event appears as a "border-line" case, while the July 3, 1998, case is certainly an extreme situation for which the behavior of the MRT and the rain rate retrieval algorithms is especially interesting to analyze. Note that with maximum estimated values of 1.5 and 0.5 dB for the June 16, 1997 and July 3, 1998 cases, respectively, the close-range attenuation effects are thought to be of limited importance for the considered rain events.

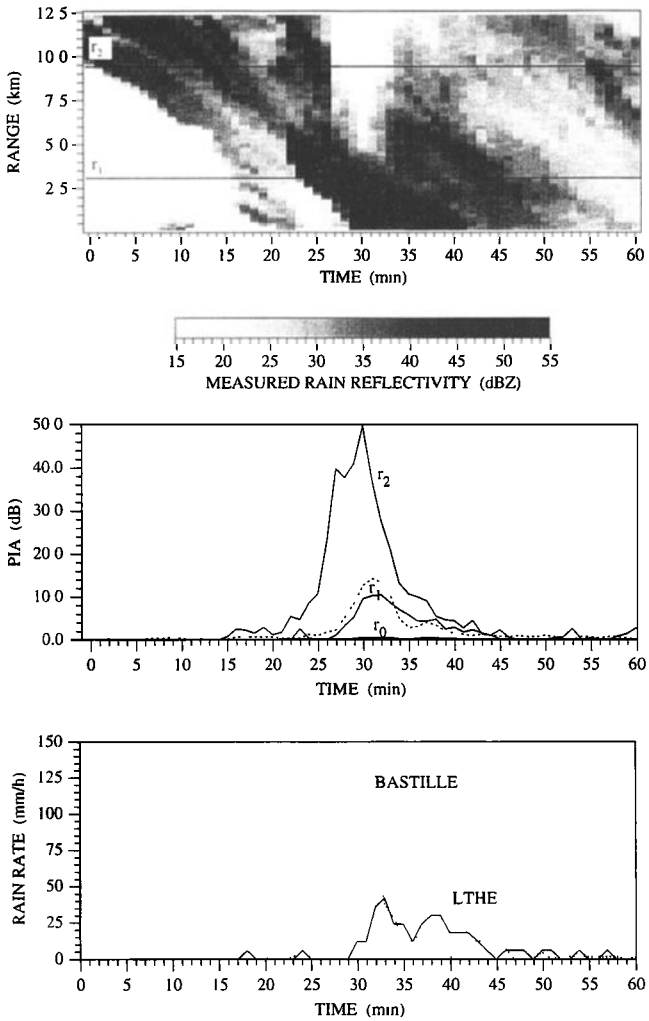

Figure 3. Same as Figure 2 for the July 3, 1998, rain event observed in the Bastille direction. This event was selected because a very impressive PIA of 50 dB was observed over a 9.5-km path using the Vercors mountain return (time step 30). Note that the two available individual rain gage hyetographs are displayed in the bottom panel instead of their average value as in Figure 2.

3. Rain Rate Retrieval for Attenuating Wavelengths

In the considered measurement context characterized by the use of an attenuated wavelength and a short range of observation (typically a couple of tens of kilometers), we may consider that instrument calibration and attenuation by rainfall are dominant sources of error in the radar measurements. From this assumption the following expression results for the measured reflectivity profile:

$$Z_m(r) = Z(r)\delta CA(r), \quad (4)$$

Table 1. Parameters of Some DSD Exponential Models Proposed in the Literature

DSD Model Name	Reference	$\Lambda(R)$, cm^{-1}	N_0, cm^{-4}	$N'_0(R)$, cm^{-4}
Widespread	*Marshall and Palmer* [1948]	$41.0\ R^{-0.21}$	0.08	$6.26 \times 10^{-2}\ R^{0.033}$
Drizzle	*Joss and Waldvogel* [1969]	$50.0\ R^{-0.21}$	0.30	$0.163\ R^{0.016}$
Widespread[a]	*Joss and Waldvogel* [1969]	$41.0\ R^{-0.21}$	0.07	$6.26 \times 10^{-2}\ R^{0.033}$
Thunderstorm	*Joss and Waldvogel* [1969]	$30.0\ R^{-0.21}$	0.014	$1.41 \times 10^{-2}\ R^{0.059}$
Brest	*Sauvageot and Lacaux* [1995]	$36.0\ R^{-0.16}$		$3.40 \times 10^{-2}\ R^{0.26}$
Cévennes	*Delrieu et al.* [1991]	$35.0\ R^{-0.215}$		$3.10 \times 10^{-2}\ R^{0.025}$
Marseille	*Delrieu et al.* [1997]	$39.9\ R^{-0.195}$		$5.40 \times 10^{-2}\ R^{0.11}$

$N'_0(R)$ is a normalized value of the parameter N_0 which guarantees the consistency of the DSD model with respect to the rain rate integral equation [*Delrieu et al.*, 1999b]. We calculated the N'_0 values using Beard's model for the terminal velocities [*Beard*, 1976] and a diameter range of 0–0.6 cm.

[a]Identical name to the Marshall and Palmer DSD model since both models have the same $\Lambda(R)$ parameter.

where $Z(r)$ ($mm^6\ m^{-3}$) is the radar reflectivity factor (termed as the reflectivity hereafter), proportional to the sum of the backscattering cross sections of the hydrometeors present per unit volume of the target. The factor δC features a possible radar miscalibration, and $A(r)$ is the two-way attenuation factor, classically expressed as a function of the attenuation coefficient k (dB km^{-1}) through the following expression:

$$A(r) = \exp\left(-0.46 \int_0^r k(s)\, ds\right). \tag{5}$$

Recall that the PIA (dB) is defined as $\mathrm{PIA}(r) = -10 \log(A(r))$. The coefficient k is proportional to the sum of the total attenuation cross sections of the hydrometeors present per unit volume. Like the reflectivity Z and the rain rate R (the useful variable for hydrological applications, classically expressed in mm h^{-1}), this coefficient therefore depends on the raindrop size distribution (DSD). When attenuating wavelengths are used, it is thus particularly important to establish (Z, k, R) relations consistent with the underlying DSDs. This problem was addressed in detail by *Delrieu et al.* [1999b]. We simply recall here that our approach is based on (1) the use of the Mie diffusion model for the backscattering and attenuation cross sections of the raindrops and (2) the description of measured DSDs using the classical negative exponential model written in the following manner:

$$N(D, R) = N_0 \exp(-\Lambda_1 R^{\Lambda_2} D). \tag{6}$$

The parameters (Λ_1, Λ_2) are fitted with DSD measurements averaged into rain rate classes, and the third parameter N_0 is calculated using the rain rate integral equation. The proposed procedure allows to derive the six parameters of the (Z, k, R) power-law relations:

$$Z = aR^b, \qquad k = cR^d, \qquad Z = \alpha k^\beta, \tag{7}$$

knowing the two parameters (Λ_1, Λ_2) of the DSD. Table 1 gives the parameters of some DSD models proposed in the literature, and Figure 4 shows the coefficients of the Z-R and Z-k relations obtained for the X band as a function of the parameters (Λ_1, Λ_2).

Three rain rate retrieval algorithms will be considered in the following: The first one, termed as the ZR method, eventually accounts for a δC calibration error prior to the simple application of the Z-R relation:

$$R^{ZR}(r) = \left(\frac{Z_m(r)}{a\,\delta C}\right)^{1/b}. \tag{8}$$

The second one, termed as the HB algorithm in reference to the well-known paper by *Hitschfeld and Bordan* [1954], performs a forward attenuation correction from range r_0 to r based on (1) the measured reflectivity profile (1) and (2) the measured close-range attenuation factor 2, through the following expression:

$$R^{HB}(r) = \left(\frac{Z_m(r)}{a((A_m(r_0)\delta C)^{1/\beta} - S_m(r_0, r))^\beta}\right)^{1/b}, \tag{9}$$

with

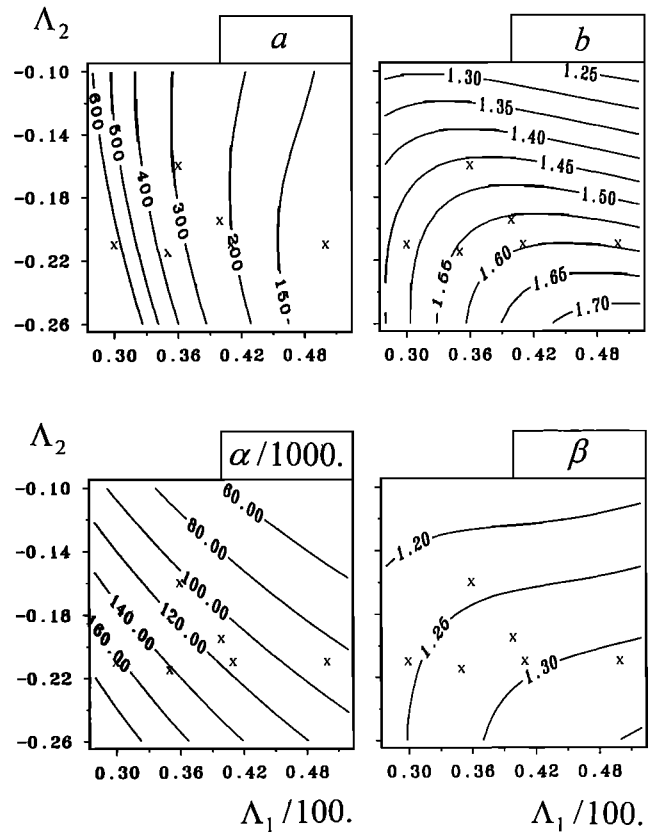

Figure 4. Evolution of the coefficients (a, b) of the Z-R power-law relation and of the coefficients (α, β) of the Z-k power-law relation in the domain defined by the (Λ_1, Λ_2) parameters of the DSD model (6) for the X band. The "cross" markers correspond to the DSD models listed in Table 1.

$$S_m(r_0, r) = \frac{0.46}{\beta} \int_{r_0}^{r} \left(\frac{Z_m(s)}{\alpha} \right)^{1/\beta} ds. \quad (10)$$

Among the surface reference technique algorithms proposed for spaceborne radar configurations, we have selected the so-called kZS algorithm [*Marzoug and Amayenc*, 1994] (MA algorithm hereinafter), which uses a mountain-derived PIA measured at a given range r_M and performs a backward correction from range r_M to range r:

$$R^{MA}(r) = \left(\frac{Z_m(r)}{a((A_m(r_M)\delta C)^{1/\beta} + S_m(r, r_M))^{\beta}} \right)^{1/b}. \quad (11)$$

Although the mathematical formulation of the two attenuation correction schemes looks rather similar, there is a fundamental difference between (9) and (11) in terms of stability. The HB algorithm is known to be very unstable due to the minus sign that appears in the denominator. It has, however, the definite advantage of being applicable in any direction of the radar detection domain, while implementation of the MA algorithm is possible only in directions, and within ranges, for which PIA measurements are available.

4. Radar Self-Calibration With the MRT

At this point we are facing the traditional dilemma of any radar data user who has to parameterize rain rate retrieval algorithms (section 3) to be applied to measured reflectivity data (section 2). Which is the representative Z-R relationship? How much is the radar miscalibration factor δC? The problem is complicated in our case because an attenuating wavelength is used (which is the representative k-R relationship?). However the available PIA measurements provide additional information compared to the nonattenuated wavelength case.

4.1. Principle of the MRT

The MRT is based on the so-called attenuation constraint equation that relates the radar measurables and three parameters of the rain rate algorithms, namely α, β, and δC. A general expression of this equation for two arbitrary ranges r_a and r_b, with $r_a \leq r_b$, can be written as follows (see DCC97 for a comprehensive derivation of this equation):

$$A_m(r_a)^{1/\beta} - A_m(r_b)^{1/\beta} \equiv \frac{S_m(r_a, r_b)}{\delta C^{1/\beta}}. \quad (12)$$

Note that in the present configuration, the interval (r_a, r_b) may correspond either to (r_0, r_1), (r_0, r_2), or to (r_1, r_2). The latter case is especially interesting since the method becomes independent of close-range attenuation effects which may be rather difficult to precisely estimate.

Assuming the three parameters $(\alpha, \beta, \delta C)$ to be constant in time and space, DCC97 have proposed to determine an optimal δC^* parameter by maximizing the consistency of the attenuation constraint equation (12) for a time series of measured reflectivity profiles and the corresponding PIAs observed during the rain event for one (or more) mountain reference target(s). A given Z-k relation has to be chosen a priori in this parameter estimation procedure. In doing so, the instrument calibration is supposed to be uncertain, and it is assumed that independent DSD measurements may provide representative (Z, k, R) relations for the rain rate retrieval algorithms. This parameter estimation procedure is similar in essence to the so-called Global Adjustment (GA) method proposed by *Amayenc and Tani* [1995] and further tested by *Marécal et al.* [1997] for an airborne radar configuration. However, assuming that the radar calibration is perfect, these authors favor the estimation of an optimal α^* parameter from which a correction term δN_0^* is derived for the multiplicative term N_0 of the DSD model. The δN_0^* term is then used to correct the multiplicative coefficients of the (Z, k, R) relations used in the rain rate retrieval algorithms.

Reality certainly lies between these two positions since radar calibration errors and biases in the parameterization of the (Z, k, R) relations probably coexist. However, being multiplicative terms in the attenuation constraint equation (see (10) and (12)), α and δC cannot be optimized individually. The ambiguity resulting of this inherent limitation of the method can partially be raised by means of a sensitivity study with respect to the DSD parameterization, as will be shown below.

4.2. Results

Some detailed considerations concerning a new mode for the practical implementation of the MRT parameter estimation procedure are presented in the Appendix. Figure 5 displays the results obtained when the estimation procedure is applied for the two rain events with a series of Z-k relations corresponding to the ranges of variation of the DSD parameters (Λ_1, Λ_2) already considered in Figure 4. The most striking result in Figure 5 is certainly the similarity of the δC^* patterns for the two rain events. This result is comforting with respect to the stability of the radar calibration during the 1-year period separating the rain events. Furthermore, the variation of the δC^* value between widespread and thunderstorm DSDs (Table 1, Figure 4) is about 1 dB with values significantly different of 0 (−2.1 and −3.3 dB, respectively). This fact attests that a significant radar calibration error is present in our case and justifies the priority that we gave to the δC^* estimation. Another important result of the DSD sensitivity study (not illustrated for the sake of conciseness) is the very low influence of the parameter β of the Z-k relation, a result also reported by *Marécal et al.* [1997].

5. Validation Using Rain Gage Data

Because of the different measurement configurations in 1997 and 1998, in particular with respect to the rain gage network, validation results are presented separately in the next paragraphs for the two rain events selected. Note that hereinafter the terms ZR1, HB1, and MA1 refer to the corresponding rain rate retrieval algorithms applied to the raw reflectivity data (that is with $\delta C = 1$), while the terms ZR2, HB2, and MA2 refer to algorithm implementations realized with the MRT-derived optimal δC^* value.

5.1. A Border-Line Case for the HB Method: June 16, 1997, Rain Event

Six rain gages located between ranges r_0 and r_1 were used for the validation of the rain rate retrieval algorithms. The validation has been performed on 5-min accumulations in order to reduce discrepancies due to the possible lack of synchronization of the various devices and to the advection of rain down to ground level. Figure 6 presents the resulting radar—rain gage scatter graphs, and Table 2 gathers the corresponding Nash criterion values. The ZR scatter graphs are characterized by a marked underestimation of most of the rain rates

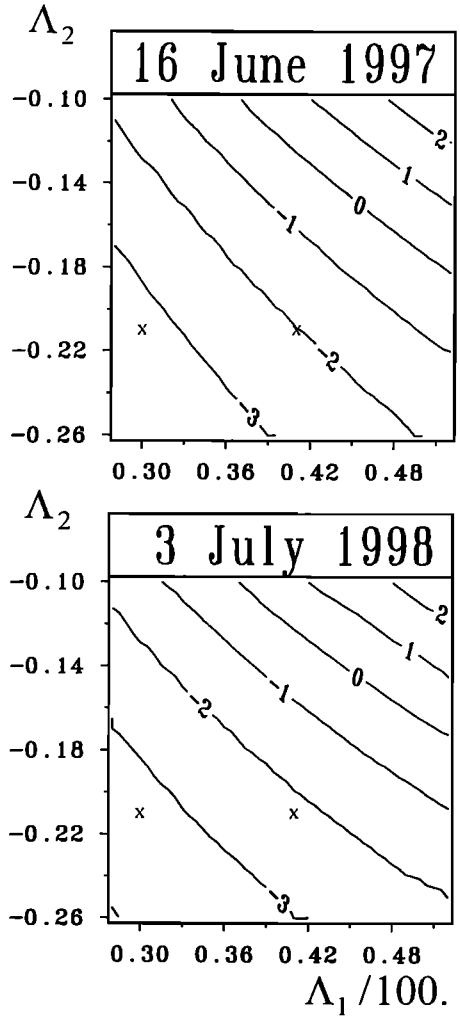

Figure 5. Sensitivity of the MRT parameter estimation procedure with respect to the DSD. The grids present the evolution of the optimal δC^* values calculated for the selected rain events when the Z-k relations derived from the displayed (Λ_1, Λ_2) DSD parameters are considered in the PIA constraint equation. The two cross markers show the so-called widespread and thunderstorm DSDs (Table 1).

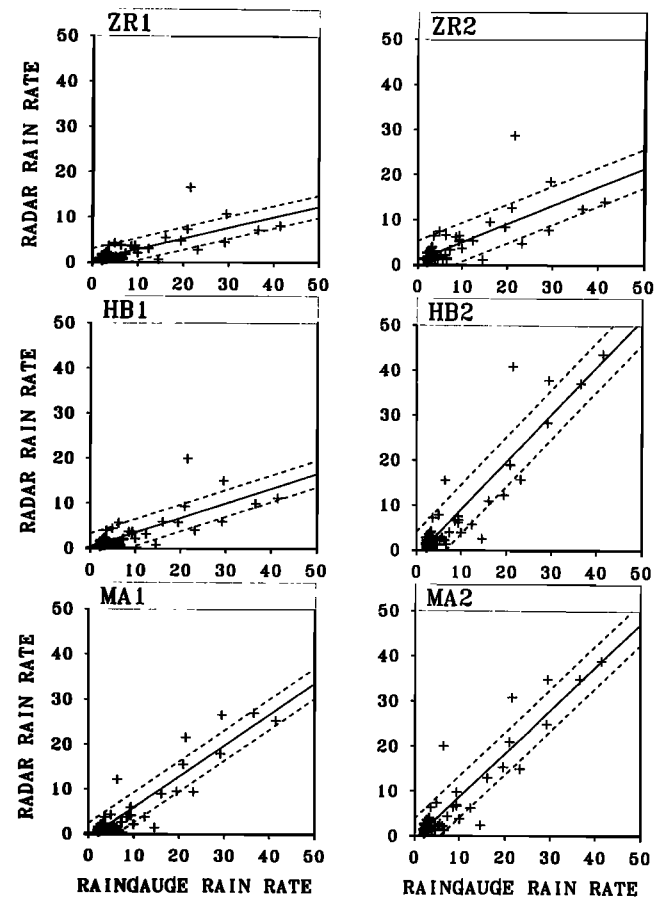

Figure 6. Validation results for the June 16, 1997, rain event. Scatter graphs of radar versus rain gage 5-min rain rate estimates (mm h^{-1}) obtained for the ZR, HB, and MA retrieval algorithms with the thunderstorm (Z, k, R) relations: $Z = 645R^{1.48}$ and $Z = 163300k^{1.24}$. The left-hand column corresponds to the results obtained with the raw reflectivity measurements, i.e., with $\delta C = 1$. The right-hand column corresponds to the results obtained with the MRT-derived optimal δC^* value (−3.4 dB). The regression line is displayed together with the corresponding 95% confidence interval (dashed lines).

greater than 10 mm h^{-1}, a clear indication of the need to correct for attenuation effects. Note that HB2 and MA2 both provide rain rate estimates that are quite well organized around the one-to-one line, while a significant underestimation remains for HB1 and MA1. It seems therefore that the MRT δC^* correction is relevant in terms of rain rate estimation. This is not a trivial result since the MRT δC^* factor is derived from the comparison of radar reflectivity and attenuation data, independently of any information on the rain rate. Note also that for this range of PIAs (that is 0–15 dB), HB2 and MA2 have about the same performance characteristics although the mountain PIA measurements are not used directly in the HB algorithm. Therefore the MRT parameter estimation procedure seems to be able to extract most of the useful information contained in the PIA measurements. Table 2 also shows that the δC^* correction is especially effective for the HB algorithm, while the MA algorithm is far less sensitive to radar calibration errors.

The sensitivity of the MRT procedure with respect to the a priori choice of the DSD and the resulting (Z, k, R) relations can be appreciated in Figure 7. The radar-rain gage validation was repeated for all the (Z, k, R) relations that can be derived from the ranges of variation of the (Λ_1, Λ_2) DSD parameters with the corresponding MRT-derived δC^* correction (Figure 5). Note that the Nash criterion patterns are quite similar for

Table 2. Validation of Rain Rate Retrieval Algorithms for the June 16, 1997, Rain Event

Rain Rate Retrieval Algorithm	1	2
ZR	−0.04	0.33
HB	0.11	0.81
MA	0.63	0.84

For each algorithm, the table lists two values of the Nash criterion corresponding to the performance obtained (1) with the raw measured reflectivity profiles; that is, with $\delta C = 1$ and 2) with the corrected reflectivity profiles by means of the optimal MRT-derived δC^* factor. The criterion estimation relies on 55 pairs of radar—rain gage values.

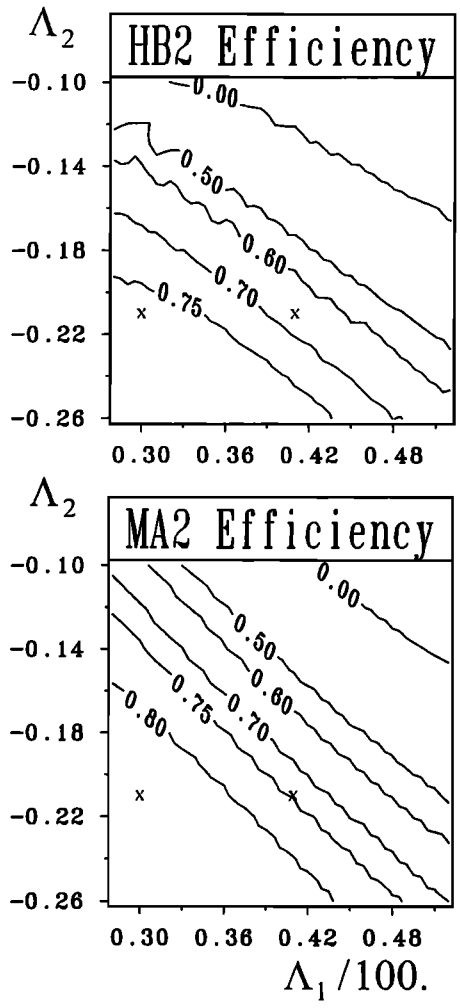

Figure 7. Sensitivity of the validation results obtained for the June 16, 1997, rain event with respect to the DSD. The grids present the evolution of the Nash criterion corresponding to HB2 and MA2 performance characteristics with respect to 5-min rain gage estimates as a function of the (Λ_1, Λ_2) DSD parameters. The rain rate retrieval algorithms are implemented with the corresponding (Z, k, R) relations and the MRT-derived optimal δC^* value displayed in Figure 5.

the two algorithms with, however, a slight superiority of MA2 with best efficiencies comprised between 0.80 and 0.85, while the best HB2 efficiencies remain less than 0.80. Efficiencies greater than 0.70 are obtained for about one third and one half of the (Λ_1, Λ_2) domain for HB2 and MA2, respectively. This result is important since it shows that the sensitivity of the MRT validation with respect to the DSD is rather low for the considered PIA range. In particular, the MRT δC^* correction seems effective in compensating both radar calibration defaults and biases related to the choice of the (Z, k, R) relations. This positive behavior is limited to reasonably realistic (Z, k, R) relations with a preference for thunderstorm relations which are certainly physically relevant for the considered rain. It cannot be extended to the right part of the (Λ_1, Λ_2) domain which corresponds to light rains.

5.2. An Extreme Case: July 3, 1998, Rain Event

For this event, the only possibility for the validation of the radar rain rate retrieval algorithms relies on the use of the Bastille rain gage. As the rain event lasted about 20 min with an intense period of 10 min only, we limit hereinafter the presentation of the results to 1-min hyetographs for a semi-quantitative assessment of the various methods (Figure 8).

The top graph clearly shows that ZR1 underestimates the Bastille rain rates after time step 27, with very severe attenuation effects between time steps 29 and 33. The 3.4 dB correction (ZR2, not shown) of the raw reflectivities derived from the MRT, which is a time-constant multiplicative correction factor of about 1.70 in terms of rain rate, is not appropriate to significantly improve the results. In the same graph, one can appreciate the HB algorithm behavior. HB1 provides quite good estimates before time step 28 but then fails for the rest of the rain event (underestimation). Conversely, HB2 provides good corrections after time step 31, but overestimations and several divergences occur between time steps 23 and 30. During this period, as mentioned in section 2, the presence of hail

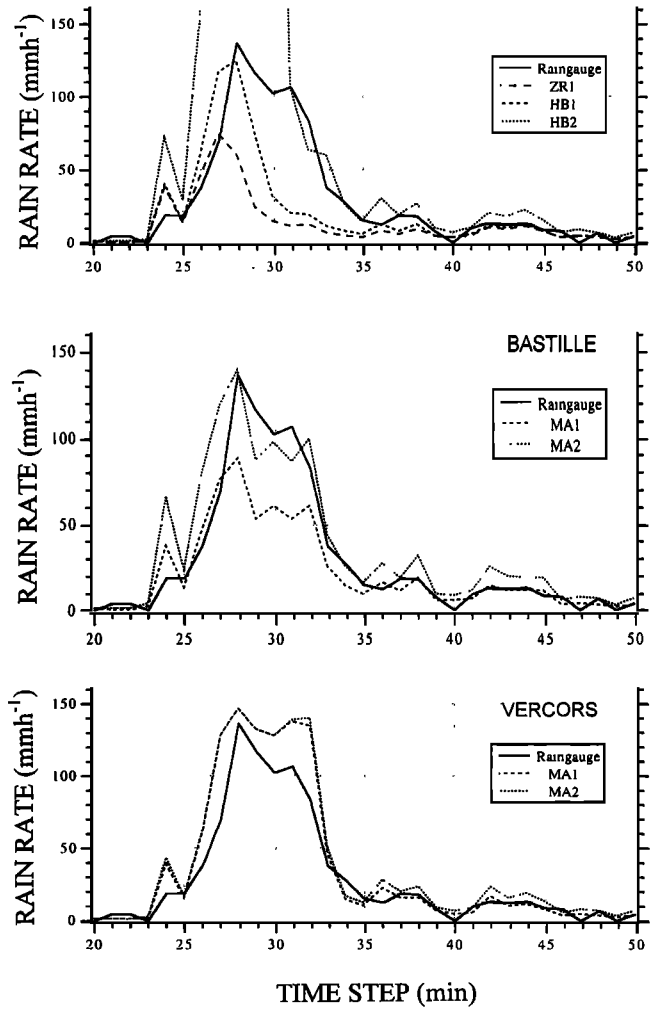

Figure 8. Validation results for the July 3, 1998, rain event in terms of rain rate estimation at the Bastille site. The three graphs allow comparison of radar rain rate retrieval algorithms with the Bastille rain gage hyetograph (solid line) with a 1-min time step. The top graph gives the results of ZR1, HB1, and HB2; the middle and the bottom graphs give the results of MA1 and MA2 applied with the Bastille and the Vercors mountains, respectively, as the reference target (see text for details).

is responsible for a sudden change of the DSD. The (Z, k, R) relations and the $|K|^2$ constant used in (1) are certainly inadequate. The definite limitation of the HB algorithm due to its basic instability is hence clearly illustrated.

The middle graph shows the results of MA1 and MA2 when the Bastille mountain is used as the reference target. In this case the right-hand term of the sum in the denominator of (11) is equal to zero since $r = r_M$. Therefore compared to the ZR method 8, the MA algorithm simply takes into account the measured attenuation at the Bastille site. This comparison is interesting since it confirms the goodness of both the MRT δC^* correction and the Z-R relation used, with a good agreement of the MA2 estimates with the rain gage values for the most intense part of the rain event (time steps 28–33). Again, the significant overestimation during the first part of the event can be attributed to the violation of the DSD time-homogeneity hypothesis in relation with the presence of hail.

Finally, in the bottom graph, MA1 and MA2 are implemented with the Vercors mountain as the reference target. This case is also instructive because it shows an example of the error-damping effect of the MA algorithm in the case of high PIA [see *Marzoug and Amayenc*, 1994]. Consideration of the denominator of (11) shows that for such attenuations (corresponding to very low attenuation factors) the influence of errors on the radar constant and on the mountain-PIA itself becomes negligible since $(A(r_M)\delta C^*)^{1/\beta}$ tends toward zero. Effectively, MA1 and MA2 provide almost identical results. Note that compared to the rain gage measurements a significant overestimation of the radar rain rates is present during the most intense part of the rain event, while the radar-rain gage agreement is remarkable during the second part of the rain event. A sensitivity study with respect to the DSD (not shown) does not yield a set of (Z, k, R) relations providing much better results.

6. Conclusion

The Mountain Reference Technique (MRT) was proposed in DCC97 as a means to calibrate a weather radar operating at an attenuated wavelength in a mountainous environment. Basically, time series of path-integrated attenuations (PIAs) derived from mountain returns and the corresponding measured reflectivity profiles are used through the so-called attenuation constraint equation to estimate an average correction factor δC^* for the radar calibration. It was shown here that for the two most important rain events of the Grenoble 97–98 Experiment the optimal δC^* factors were almost equal to each other, a comforting result with respect to the stability of the radar instrument during the corresponding 1-year period. Compared to DCC97, an improved scheme was proposed for the MRT parameter estimation procedure with a more satisfactory treatment of high-attenuation effects (Appendix). A "differential" form of attenuation constraint equation was also proposed when two reference targets are available in a given direction of the detection domain. In such a configuration the MRT becomes independent of close-range attenuation effects that occur within the range r_0 where the reflectivities are noisy due, for instance, to sidelobe contamination. Note also that because of the accuracy of mountain-derived PIAs (DSGC99) we recommend to use only PIA values greater than about 3 dB in the MRT parameter estimation procedure.

Compared to standard radar calibration techniques based on rain gage data, the definite advantage of the MRT is to rely on radar data alone. However, like these other techniques, the MRT imposes the a priori choice of a DSD model and of the subsequent (Z, k, R) relations. Although the MRT is based on reflectivity and attenuation measurements only, validation of the rain rate retrieval algorithms with respect to rain gage data for the June 16, 1997, rain event showed that this technique is relevant in terms of rain rate estimation. Furthermore, when realistic models are considered for the DSD, the δC^* factor allows to compensate for moderate biases related to the choice of the (Z, k, R) relations. For this rain event, with maximum PIA values of about 15 dB, the HB and the MA algorithms were found to provide equivalent results when the δC^* factor was accounted for, a confirmation of the Marseille validation results (DCC97). However, the July 3, 1998, case (maximum PIA of 50 dB over a 9-km propagation path and presence of hail at the beginning of the storm) clearly shows that the HB algorithm, even if it is implemented with the optimal δC^* factor, cannot correct for such high-attenuation effects because of its inherent instability [*Delrieu et al.*, 1999b]. For this event the MA algorithm proved to be remarkably stable and efficient in terms of rain rate estimation in comparison to the Bastille rain gage. These interesting features are counterbalanced by the fact that the MA algorithm implementation is limited to directions for which PIA measurements are available.

A final implication of the present work concerns the radar-scanning strategy. The MRT is worth being applied on data collected in RHI mode. In this case, the mountain-derived PIAs and the corresponding measured reflectivity profiles are synchronous, an important condition for increasing the attenuation constraint equation consistency. Furthermore, RHIs are useful to detect some of the phenomena that may limit the validity of the method (presence of rain at the radar site or over the reference target, vertical heterogeneity of the reflectivities such as bright band, etc). Therefore a possible future scan strategy for our radar system could be made of (1) PPIs at various elevation angles to obtain the best possible visibility over the detection domain and (2) RHIs in the direction of various selected ground reference targets to implement the MRT and, at the same time, obtain a detailed characterization of the vertical structure of the atmosphere.

Appendix: New Implementation Mode for the MRT Estimation Procedure

In the Marseille case study (DCC97) the δC optimization was performed using the following form of the attenuation constraint equation:

$$\mathrm{PIA}_c(r_b) = -10\beta \log\left(A_m(r_a)^{1/\beta} - \frac{S_m(r_a, r_b)}{\delta C^{1/\beta}}\right). \quad \text{(A1)}$$

The PIAs calculated from (A1) were compared to the measured mountain-derived $\mathrm{PIA}_m(r_b)$, and the optimal δC^* value was determined using the efficiency, or Nash criterion, as the likeness criterion between the two series. The use of (A1) in the correlation analysis is justified because it gives more weight to high-attenuation effects. However, consideration of this equation shows that an estimation of $\mathrm{PIA}(r_b)$ can be obtained only if

$$S_m(r_a, r_b) < (\delta C A_m(r_a))^{1/\beta}. \quad \text{(A2)}$$

In the practical implementation of the method the number of points for which this condition is not met increases as δC

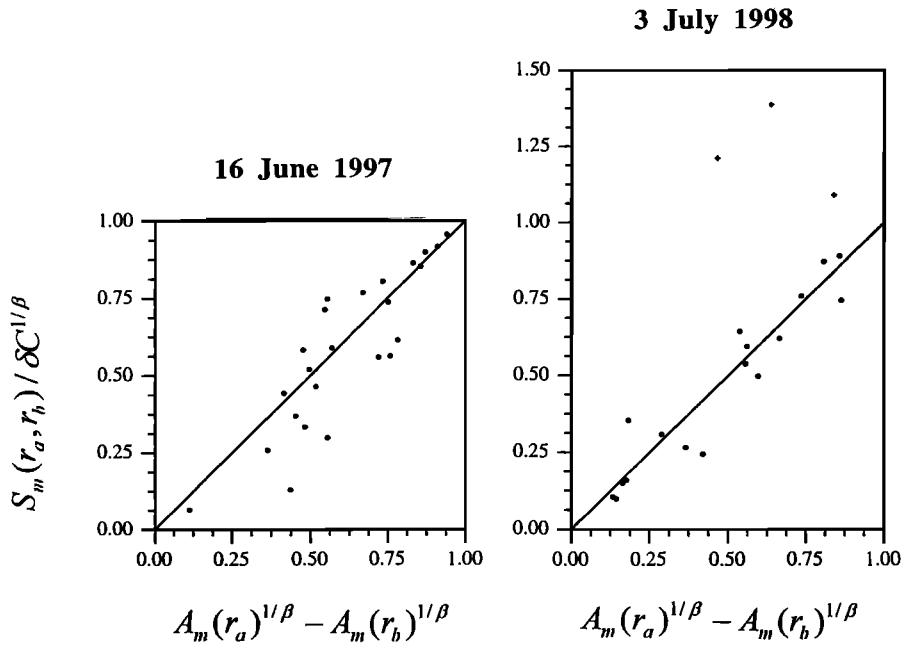

Figure A1. Illustration of the MRT parameter estimation procedure: consistency of the PIA constraint equation (12) for the June 16, 1997 (left) and the July 3, 1998 (right), rain events. The optimal δC^* values (i.e., −3.4 and −3.3 dB, respectively) obtained for the thunderstorm Z-k relation ($Z = 163300k^{1.24}$) are accounted for in the calculation of the displayed values. For the July 3, 1998, rain event, note that the three plusses for which constraint (A2) is not satisfied are excluded from the Nash criterion evaluation for this particular δC value.

decreases. This fact poses a problem concerning the way these "divergences" (indeed, the fact that (A2) is not satisfied corresponds to a divergence of the attenuation correction based on the Hitschfeld and Bordan's formulation (9)) are accounted for in the procedure. We proposed in DCC97 to set the corresponding calculated PIAs to an artificially high value (e.g., 100 dB) and to account for them in the correlation analysis in order to penalize the corresponding values of δC. However, the study of the July 3, 1998, case showed that some divergences can be observed for a δC value, which is optimal for the vast majority of points of comparison. Therefore we propose here a new mode for the implementation of the attenuation constraint equation based directly on equation (12). Although there is no mathematical restriction in the calculation of the two members of (12), the correlation analysis is performed, for each δC value, over a set of points, denoted $N - N_{\text{div}}(\delta C)$, where N is the total number of cases, and $N_{\text{div}}(\delta C)$ is the number of cases for which (A2) is not satisfied. To account for the PIA measurement accuracy, two conditions are actually considered in the selection of the points: (1) a tolerance is made in the determination of $N_{\text{div}}(\delta C)$ using (A2) since the attenuation factor $A(r_a)$ is replaced by $A_m(r_a)10^{\delta \text{PIA}_M/10}$, where $A_m(r_a)$ is the measured attenuation factor and δPIA_M is the accuracy of the mountain PIA (taken to be +2.5 dB in the present case, after DSGC99); (2) N is taken as the number of points for which the PIAs (and the differences in PIAs between the two ranges) are greater than δPIA_M.

Figure A1 illustrates the proposed method for the two selected rain events. For these calculations a thunderstorm Z-k relation was used for both events. Furthermore, the points corresponding to the (r_0, r_1) and (r_1, r_2) range intervals were grouped in order to increase the reliability of the optimization. Note that for the July 3, 1998, rain event the consistency of the attenuation constraint equation is remarkable for the $N - N_{\text{div}}(\delta C^*)$ points. The three outliers seem to correspond to a temporary violation of the DSD homogeneity hypothesis. They appear consecutively during the first part of the storm and are characterized by unusually high reflectivities with respect to the resulting PIAs. The presence of hail, which was reported at ground level at the Bastille site (section 2), probably explains such a behavior (see (1) and the values of $|K|^2$ for water and ice).

Acknowledgments. Thanks are due to J. M. Taunier, F. Cazenave, S. Boubkraoui, F. el Ouazzany, A. Bdéoui, and T. Pellarin (LTHE) for their participation in the Grenoble 97–98 measurement campaign. We are also indebted to the "Mairie de Saint Jean le Vieux" and the "Institut de Géographie Alpine" for allowing us to install and operate the receiving antenna in 1997 and 1998, respectively. The comments of three anonymous reviewers were very helpful in making this paper clearer and more concise. This study received financial support of the French "Ministère de l'Aménagement du Territoire et de l'Environnement" (Programme: Utilisation des radars météorologiques pour l'annonce des crues et la gestion des réseaux d'assainissement), of the "XIième Contrat de Plan Etat-Région Rhônes-Alpes" (Programme de recherche sur les risques naturels) and of the Environment and Climate Program of the European Community (HYDROMET project, grant ENV4CT96-0290).

References

Amayenc, P., and T. Tani, Tests of algorithms for range-profiling of the rain rate from ARMAR in TOGA-COARE, in *Preprints, 27th Conference on Radar Meteorology*, pp. 789–791, Am. Meteorol. Soc., Boston, Mass., 1995.

Beard, K. V., Terminal velocity and shape of cloud and precipitation drops aloft, *J. Atmos. Sci.*, *33*, 851–864, 1976.

Delrieu, G., J. D. Creutin, and I. Saint-André, Mean K-R relationships: Practical results for typical weather radar wavelengths, *J. Atmos. Oceanic Technol.*, *8*, 467–476, 1991.

Delrieu, G., S. Caoudal, and J. D. Creutin, Feasibility of using moun-

tain return for the correction of ground-based X-Band weather radar, *J. Atmos. Oceanic Technol.*, *14*, 368–385, 1997.

Delrieu, G., S. Serrar, E. Guardo, and J. D. Creutin, Rain measurement in hilly terrain with X-band radar systems: Accuracy of mountain-derived path-integrated attenuations, *J. Atmos. Oceanic Technol.*, *16*, 405–416, 1999a.

Delrieu, G., L. Hucke, and J. D. Creutin, Attenuation in rain for X- and C-band weather radar systems: Sensitivity with respect to the drop size distribution, *J. Appl. Meteorol.*, *38*, 57–68, 1999b.

Doviak, R. J., and D. S. Zrnic, *Doppler Radar and Weather Observations*, 562 pp., 2nd ed., Academic, San Diego, Calif., 1993.

Hitschfeld, W., and J. Bordan, Errors inherent in the radar measurement of rainfall at attenuating wavelengths, *J. Meteorol.*, *11*, 58–67, 1954.

Joss, J., and A. Waldvogel, Raindrop size distribution and sampling size error, *J. Atmos. Sci.*, *26*, 566–569, 1969.

Marécal, V., T. Tani, P. Amayenc, C. Klapisz, E. Obligis, and N. Viltard, Rain relations inferred from microphysical data in TOGA COARE and their use to test a rain-profiling method from radar measurements at Ku-band, *J. Appl. Meteorol.*, *38*, 1629–1646, 1997.

Marshall, J. S., and W. K. Palmer, The distribution of raindrops with size, *J. Meteorol.*, *5*, 165–166, 1948.

Marzoug, M., and P. Amayenc, A class of single and dual-frequency algorithms for rain rate profiling from a spaceborne radar, part 1, Principle and tests from numerical simulations, *J. Atmos. Oceanic Technol.*, *11*, 1480–1506, 1994.

Meneghini, R., J. Eckerman, and D. Atlas, Determination of rain rate from a spaceborne radar using measurements of total attenuation, *IEEE Trans. Geosci. Remote Sensing*, *GE-21*, 34–43, 1983.

Sauvageot, H., and J. P. Lacaux, The shape of averaged drop size distributions, *J. Atmos. Sci.*, *52*, 1070–1083, 1995.

J.-D. Creutin, G. Delrieu, S. Serrar, and R. Uijlenhoet, LTHE, UMR 5564 (CNRS, UJF, INPG, ORSTOM), BP53, F-38041 Grenoble Cedex 9, France. (guy.delrieu@hmg.inpg.fr)

(Received February 25, 1999; revised August 30, 1999;
accepted September 27, 1999.)